SLAC-PUB-2052
December 1977
(T/E)

CORRELATIONS BETWEEN LEADING PROTONS AND LARGE TRANSVERSE MOMENTUM PARTICLES AND BETWEEN LEADING PROTONS AND MASSIVE LEPTON PAIRS IN THE QUARK-PARTON MODEL*

J. Ranft†

Stanford Linear Accelerator Center
Stanford University, Stanford, California 94305

ABSTRACT

Correlations between leading protons, produced in proton collisions and large $p_\perp$ particles and between leading protons and massive lepton pairs are studied using the quark parton model. The leading proton production is described according to a valence quark recombination mechanism, large $p_\perp$ jets are produced by the hard scattering of quark partons and lepton pairs are produced according to the Drell-Yan mechanism. The predictions of the quark recombination mechanism agree well with leading proton, neutron and Λ-hyperon distributions in low $p_\perp$ events. The predicted correlations between leading protons and large $p_\perp$ particles agree well with recent experimental data. Strong correlations are also predicted between leading protons and massive lepton pairs. The further experimental and theoretical study of such correlations is expected to contribute to the confirmation or exclusion of proposed production mechanisms.

(Submitted to Phys. Rev. D)

---

*Work supported by Department of Energy.

†Permanent address: Sektion Physik, Karl-Marx-Universität
Leipzig, G.D.R.

I. INTRODUCTION

Particle production at large transverse momentum in hadron hadron collisions is currently being interpreted as evidence for the hard scattering of constituents. While there are several competing hard collision models,[1] it would be most natural if the interacting constituents would be the quark-partons known from deep inelastic lepton hadron interactions. Indeed, this model was the first to be proposed[2] and worked out in detail.[3] However, present data do not agree with the $p_\perp^{-4}$ behaviour of the model, which is only weakly modified by taking the QCD hard scattering cross section and using quark distribution functions which deviate--as predicted by asymptotic freedom--from Bjorken scaling.[4,5] Quark-quark scattering models with phenomenological hard scattering cross sections leading to the $p_\perp^{-8}$ behaviour were recently quite successful in describing the majority of the experimental data available.[6,7]

The longitudinal momentum distribution of leading protons as observed in low $p_\perp$ hadron-hadron collisions were first interpreted by Pokorski and Van Hove[8] as due to the recombinations of the three valence quarks of the original proton. The relevance of quark-partons for the particle production in the fragmentation region was discussed repeatedly.[9] Recently Das and Hwa[10] explained the production of mesons in the fragmentation region of p p collisions as due to the recombination of quark-partons.

If both, leading particles as well as large $p_\perp$ jets are related to constituent valence quarks of the incoming protons, it is natural, to ask for correlations between leading protons and large $p_\perp$ jets within this model. In the present paper we study such correlations using the quark recombination model for the leading proton production and the quark-quark scattering model for the large $p_\perp$ particle production. Experimental data indicating the presence of strong correlations

between forward going positive particles and positively as well as negatively charged large $p_\perp$ trigger particles are due to the British-French-Scandinavian-ISR collaboration.[11]

Better established, than for the production of large $p_\perp$ particles, is the production mechanism of massive lepton pairs in hadron-hadron collisions. There is now rather strong evidence that the Drell-Yan quark-antiquark annihilations mechanism[12] explains the experimental data available.[13] In view of this the case, to study the correlations between leading protons and massive lepton pairs is even stronger. So far no experimental evidence for such correlations is available, but strong correlations between leading protons and massive lepton pairs are predicted in our approach.

The experimental study of both kinds of correlations as well as of similar ones is expected to become a powerful tool in order to establish or exclude proposed production mechanisms for large $p_\perp$ particles, heavy lepton pairs, new heavy particles, leading particles, etc.

In Section 2 we will describe the quark recombination model for leading baryons and compare the Feynman x distributions obtained with data on inclusive proton, neutron and Λ-Hyperon production in the fragmentation region of proton-proton collisions.

In Section 3 the correlations between leading protons and large $p_\perp$ quark jets are studied and compared with recent ISR-data. In Section 4 we study the correlations between massive lepton pairs and leading protons. The expected features of these correlations are discussed. Finally in Section 5 our conclusions are presented.

II. QUARK RECOMBINATION INTO LEADING BARYONS

As shown recently by Das and Hwa,[10] the production of mesons in the fragmentation region of proton-proton collisions, can be well described by quark-antiquark recombination. Here we extend this method to describe single particle distributions of leading baryons in proton-proton collisions.

Let us first describe the method of Das and Hwa:[10] we consider the recombination of a π^+ meson out of an u valence quark and a $\bar{d}$ sea quark. The inclusive π^+ production cross section in the fragmentation region is obtained as

$$\frac{d\sigma}{dx} = \int \frac{dx_1}{x_1} \frac{dx_2}{x_2} F(x_1, x_2) R(x_1, x_2, x) \qquad (2.1)$$

Here x is the Feynman x of the pion, x_1 and x_2 are the momentum fractions of the u and d quarks, $F(x_1, x_2)$ is the two quark distribution function and $R(x_1, x_2, x)$ is a recombination function.

The quark-antiquark recombination function is assumed to scale in $\xi = x_i/x$ and it is assumed that the recombination of just one quark-antiquark pair dominates. Das and Hwa[10] use the simple symmetric form

$$R(\xi_1, \xi_2) = \alpha_\pi \xi_1 \xi_2 \delta(\xi_1 + \xi_2 - 1) \quad . \qquad (2.2)$$

The constant parameter α_π is determined from the sum rule

$$\int_0^1 d\xi_1 \int_0^1 d\xi_2 \, R(\xi_1, \xi_2) = 1 \qquad (2.3)$$

as $\alpha_\pi = 6$.

The two quark distribution function $F_2(x_1, x_2)$ is assumed to behave like

$$F_2(x_1, x_2) = \beta F_{u,val}(x_1)\, F_{\bar{d}}(x_2)(1-x_1-x_2) \tag{2.4}$$

where the $F_i(x)/x$ are the single quark distributions and β is a constant.

Inserting (2.2) and (2.4) into the expression (2.1) we obtain

$$\left.\frac{d\sigma}{dx}\right|_{\pi^+} = \alpha_\pi \beta \frac{1-x}{x} \int_0^x dx_1 \; F_{u,val}(x_1) F_{\bar{d}}(x-x_1) \tag{2.5}$$

Das and Hwa[10] find that the production of π^+, π^-, K^+ and K^- in the fragmentation region is well described by this method. All sea quark distributions are used with the same x dependence $s(x) \sim (1-x)^7$ but in order to describe the normalizations of the meson distributions, different normalizations at x = 0 are needed.

$$\frac{\bar{d}(0)}{\bar{u}(0)} = 1.35 \qquad \frac{\bar{s}(0)}{\bar{d}(0)} = 0.11 \tag{2.6}$$

In the following we generalize the recombination mechanism to describe leading baryon distributions in proton proton collisions. Following Van Hove and Pokorski[8] we assume the leading protons in proton-proton collisions to result from the recombinations of the three valence quarks. For the production of a leading neutron, one of the u valence quarks is replaced by a d-sea quark. For Λ hyperon production, one of the u-valence quarks is replaced by a s-sea quark. For the inclusive single particle distribution of non-diffractively produced protons we write analogously to (2.1).

$$\left.\frac{d\sigma}{dx}\right|_p = \int \frac{dx_1}{x_1}\frac{dx_2}{x_2}\frac{dx_3}{x_3} F_3(x_1, x_2, x_3)\, R_3(x_1, x_2, x_3, x) \tag{2.7}$$

Here x is the Feynman variable $x = 2p_\parallel/\sqrt{s}$ of the proton, the x_i are the momentum fractions of the three quarks, $F_3(x_1, x_2, x_3)$ is the three valence quark distribution in

the proton and R_3 is the three quark recombination function.

We assume the three quark recombination function to scale in the $\xi_i = x_i/x$. All contributions resulting from the recombinations of more than three quarks are assumed to be negligable. We use

$$R_3(x_1, x_2, x_3, x) = \alpha_p \xi_1 \xi_2 \xi_3 \delta(\xi_1+\xi_2+\xi_3-1) \tag{2.8}$$

The parameter α_p is obtained from the sum rule

$$\int_0^1 d\xi_1 \int_0^1 d\xi_2 \int_0^1 d\xi_3 R(\xi_1, \xi_2, \xi_3) = 1 \tag{2.9}$$

as $\alpha_p = 120$.

Next we need a parametrization of the three quark distribution $F_3(x_1, x_2, x_3)$. For the applications in Section 3 and 4 it would be most useful to write $F_3(x_1, x_2, x_3)$ in a form containing the single valence quark distributions $F_i(x_i)$ explicitly. Otherwise, integrating over the x variables of two of the quarks the single quark distribution should be obtained

$$F(x_1) = \int_0^{1-x_1} dx_2 \int_0^{1-x_1-x_2} dx_3 F_3(x_1, x_2, x_3) \tag{2.10}$$

This condition excludes, because of the integration limits a simple factorized form. The condition (2.10) is however approximately fulfilled in most of the x_1 region by choosing

$$F_3(x_1, x_2, x_3) = \beta_p F_{u,val}(x_1)\, F_{u,val}(x_2)\, F_{d,val}(x_3)(1-x_1-x_2-x_3)^{\gamma} \tag{2.11}$$

with a suitably chosen power γ. Excluding the region $0.95 \leq x_1 \leq 1$ we find the condition (2.10) to be fulfilled best with $\gamma = -0.3$.

Inserting (2.8) and (2.11) into (2.7) we obtain

$$\left.\frac{d\sigma}{dx}\right|_p = \alpha_p \cdot \beta_p \frac{(1-x)^\gamma}{x^2} \int_0^x dx_1 F_{u,val}(x_1) \int_0^{x-x_1} dx_2$$

$$\cdot F_{u,val}(x_2) F_{d,val}(x-x_1-x_2) \qquad (2.12)$$

Replacing in (2.12) one of the u valence quark distributions by the d or s sea quark distribution, we obtain the neutron and Λ-hyperon distributions.

The resulting inclusive proton, neutron and Λ-hyperon production cross sections $d\sigma/dx$ are plotted in Figures 1 and 2 and compared with experimental data. We find only small differences of the calculated x-distributions using different parametrizations for the quark distribution functions.[14, 15, 6] The curves plotted in Figures 1 and 2 were obtained using the parametrization of Field and Feynman.[6] Likewise, the power γ in (2.11) within the range of its uncertainty has only small influence on the shape of the obtained distributions.

In Figure 1 we compare the $d\sigma/dx$ cross section with data of Chapman et al.[16] on proton production at 102 and 405 GeV and with data on Λ-production form experiments at 69 to 300 GeV/c.[17] While the proton production is well understood in its absolute normalizations with a parameter $\beta_p \approx 0.5$, we used for the normalization of the Λ-distribution to agree with experiment a suppression factor for strange sea quarks $\bar{s}/\bar{d} \approx 0.1$, this compares well with the corresponding factor (2.6) found by Das and Hwa[10] from Kaon production. In Figure 2 we compare inclusive single particle cross sections $E\, d^3\sigma/d^3p$ at fixed transverse momentum with ISR data on proton production at $\sqrt{s} = 31$ GeV and $p_\perp^2 = 0.275$ $(GeV/c)^2$ from Albrow et al.[18] and with data on neutron production at $\sqrt{s} = 30.6$, 44 and 53 GeV at $p_\perp = 0.4$ and 0.6 GeV/c from Engler et al.[19] We assume in the comparison, that the longitudinal momentum distribution and transverse momentum distributions factorize

approximately. The relative normalization of the calculated curves for proton and neutron production are as obtained in the calculation and is consistent with the experimental data, note that the proton and neutron data are for different $p_\perp$ values!

From the overall agreement of the calculated leading baryon distributions with data, we might conclude, that the recombination of the leading proton out of 3 valence quarks--a choice, which is by no means unique, for an alternative approach see Ref. 20-- is not contradicted by the data. We might also hope to explain in this scheme the correlations of leading protons with large $p_\perp$ particles successfully, In calculating the neutron cross sections, we replace one valence quark of the proton by one sea quark, the same replacement is necessary to calculate the leading proton distribution when one of the valence quarks of the original proton is elastically scattered to form a large $p_\perp$ jet.

III. CORRELATIONS BETWEEN LARGE $p_\perp$ JETS AND LEADING PROTONS

The correlation between large $p_\perp$ jets and leading protons could be calculated within different hard collision models. We choose here the quark-quark scattering model to describe large $p_\perp$ jet production, because it seems to be most straightforward to consider in this model the correlation to leading protons which are calculated with the quark recombination mechanism as described in Section 2. Furthermore, the quark distributions needed in this model are well known from deep inelastic lepton-proton collisions and large $p_\perp$ single particle distributions and correlations are well described by this model.[6,7]

There are two different mechanisms, which lead to correlations between large $p_\perp$ jets and leading particles.

(i) Kinematic correlations: In events with a large $p_\perp$ trigger particle, less energy is available for leading particles. Therefore, we expect a suppression

of leading particle production in all models. In addition to this kinematic effect we expect some change in the leading particle production in the presence of a large $p_\perp$ jet around $\theta \approx 90^o$ in the cms due to the suppression of diffractive events by the trigger.

(ii) Dynamical correlations: Large $p_\perp$ jets in the quark-quark scattering model result mostly from the hard scattering of valence quarks of the incident protons. These valence quarks are no longer available for the recombination into leading protons. Leading protons are created at a reduced rate by the recombination of the remaining 2 valence quarks with one sea quark, see Figure 3a. This dynamical effect leads to stronger correlations then expected due to the kinematical mechanism only.

We calculate the joint distribution of one large $p_\perp$ quark jet and one leading proton according to Figure 3. The hard scattering involves one valence quark of the incoming proton A (Figure 3a) or one sea quark (Figure 3b). In the first case the proton is recombined out of 2 valence quarks and one sea quark, in the second case it is recombined out of the 3 valence quarks. At a sufficiently large $p_\perp$ the hard scattering of valence quarks, Figure 3a dominates. We denote energy, momentum and angle of the scattered final state quark jet by E_k, p_k, and θ_k and the Feynman x of the leading proton by x. The expression for the joint jet-leading proton distribution is

$$E_k \frac{d^4\sigma}{d^3p_k dx} \approx \frac{2}{\pi} \sum_j \int_{x_0}^{1} \frac{dx_1}{2x_1 - \cot\left(\frac{\theta_k}{2}\right) y_\perp} F_k(x_1) F_j(x_2) \frac{d\sigma}{d\hat{t}} \cdot H_k\left(\frac{x}{1-x_1}, x_1\right)$$

$$+ \text{ term with } \frac{d\sigma}{d\hat{u}} \qquad (3.1)$$

with definitions of the variables:

$$x_0 = \frac{y_\perp \cot\frac{\theta_k}{2}}{2 - y_\perp \operatorname{tg}\frac{\theta_k}{2}} \leq x_1 \leq 1$$

$$x_2 = \frac{x_1 \operatorname{tg}^2\frac{\theta_k}{2}}{\eta}$$

$$\eta = \frac{2 \operatorname{tg}(\frac{\theta_k}{2}) \cdot x_1 - y_\perp}{y_\perp} \qquad (3.2)$$

$$\hat{t} = -\frac{x_1 s\, y_\perp}{2} \operatorname{tg}\frac{\theta_k}{2}$$

$$y_\perp = \frac{2p_\perp k}{\sqrt{s}}$$

The function $H_k(x, x_1)$ describes the single particle distribution of the leading proton out of the quarks u, v and w similarly as given by Eq. (2.12).

We take energy momentum conservation into account by replacing the argument x of H by $x/(1-x_1)$. In this way the maximum x of the leading proton becomes $1-x_1$ as demanded by energy-momentum conservation. Furthermore we have to consider that the quark k (in the $d\sigma/dt$ term) has been scattered out of the incoming proton. If k is a u or d quark, the probability for being a valence quark is

$$\alpha(x_1) = \frac{F_{k,\,val}(x_1)}{F_{k,\,val}(x_1) + F_{k,\,sea}(x_1)} \qquad (3.3)$$

correspondingly, $(1-\alpha(x_1))$ is the probability for k being a sea quark. According

to this we write

$$H_k(x,x_1) = \alpha_p \beta_p \frac{(1-x)^\gamma}{x^2} \int_0^x dx_u F_{u,val}(x_u) \cdot$$

$$\int_0^{x-x_u} dx_v F_{v,val}(x_v) \Big[\alpha(x_1) F_{w,sea}(x-x_u-x_v)$$

$$+ \big(1-\alpha(x_1)\big) F_{w,val}(x-x_u-x_v) \Big] \qquad (3.4)$$

In order to present the large $p_\perp$-leading proton correlation we define a divided correlation function similarly as used frequently to study short range correlations of low $p_\perp$ particles.[21] This correlation function was also used to present the only experimental data available so far.[11] We define

$$R(p_{\perp k}, y_k, x) = \frac{E_k \frac{d^4\sigma}{d^3p_k dx}}{E_k \frac{d^3\sigma}{d^3p_k} \cdot \frac{d\sigma}{\sigma dx}} - 1 \qquad (3.5)$$

It is $E_k d\sigma/d^3p_k$ the inclusive distribution of large $p_\perp$ quark jets and $d\sigma/dx$ the leading particle density.

In order to study the kinematic contribution to the correlation function (3.5) separately, we calculate the distribution (3.1) and the single jet distribution for the case that only sea quarks contribute to the hard scattering process.

In the actual calculations we use again the quark distribution functions in the parametrizations according to Field and Feynman.[6] We restrict the calculation and compare with data only for leading particles with $x > 0.4$ to 0.5. At these x

values positive secondaries are dominantly protons. The calculated correlation function $R(p_\perp, y, x)$ is plotted in Figures 4 and 5, where we also compare with experimental data from the British-French-Scandianvian ISR-Collaboration.[11] The calculated cross sections refer to large $p_\perp$ quark jet production, the experimental data are for negatively and positively charged large $p_\perp$ trigger particles, which we might interpret as mainly pions. We calculate the cross sections and correlation functions separately for u- and d-quark jets; u-quarks fragment dominantly into positively charged large $p_\perp$ trigger particles, d-quarks will fragment mainly into negatively charged triggers. The transverse momenta of the observed trigger particles are smaller than the transverse momenta of the quark jets. This question was studied in detail in connection with trigger bias effects.[22, 23, 24] In our comparison we assume that 2/3 of the jet momentum is carried by the fastest trigger particle. Recent parametrizations of the quark-fragmentation functions[6] lead to somewhat larger fractions. A corresponding change would not change our conclusions significantly.

In Figures 4a and b we plot the correlation functions vs the Feynman x of the leading proton. In Figures 5a and b we plot it vs. the trigger $p_\perp$. In Figures 4a and 5a we compare the data with the full calculated correlation function, which includes the kinematic as well as dynamic correlations. In Figures 4b and 5b we compare with only the kinematic correlations calculated according to Figure 3b for processes involving only the hard scattering of sea quarks. While the curves in Figures 4a and 5a agree quite well with the data, we find that the kinematic correlations alone are not able to explain the observed suppression of the joint leading particle-large $p_\perp$ production.

In Figure 6 we show the calculated correlation function vs. the jet transverse momentum for different values of the cms jet rapidity. At positive jet rapidities

the jet moves also forward and uses a larger fraction of the available collision energy, furthermore it is more likely to result from a forward moving valence quark. Correspondingly the correlation function decreases rapidly when the jet rapidity is increased.

We conclude: there are strong correlations between leading protons and large $p_\perp$ particles which can be well understood within the model studied. Such correlations are expected to contribute significantly to the further confirmation and/or exclusion of proposed production mechanisms. It is reassuring to see also that the difference between the correlation functions for positive and negative trigger particles is well understood in the model as due to the difference between the u- and d-valence quark distribution functions. We point out, that similar specific correlation effects are likely to occur if the correlation function is studied for identified large $p_\perp$ trigger particles and identified leading particles.

IV. CORRELATIONS BETWEEN MASSIVE LEPTON PAIRS PRODUCED IN pp COLLISIONS AND LEADING PROTONS

The production of massive lepton pairs, e^+e^- or $\eta^+\eta^-$ in hadron-hadron collisions is generally assumed to proceed according to the Drell-Yan mechanism.[12] Increasing experimental evidence indicates, that this indeed seems to be the correct production mechanism. The interpretation of massive lepton pair production via quark-antiquark annihilation is now much safer than the interpretation of large transverse momentum particle production, where still several competing mechanisms are possible.

It is therefore natural, to study the correlations between leading protons and massive lepton pairs in the hope to understand in more detail the quark recombination mechanism of the leading particle production, to confirm further the Drell-Yan mechanism and to understand better the production mechanisms and quantum

number correlations in large $p_\perp$ processes and in the production of heavy new particles like the J, ψ.

In this spirit, we propose in the following, to observe one single on both leading protons simultaneously with heavy lepton pairs and predict the characteristics of the correlations in this case. We describe the lepton pair by the scaling variable

$$\tau = \frac{M^2}{s} = x_1 \cdot x_2 \tag{4.1}$$

and by the Feynman variable x_M for the lepton pair

$$x_M = x_1 - x_2 \quad . \tag{4.2}$$

where M^2 is the squared mass of the heavy lepton pair, s is the square of the c.m.s. energy and x_1 and x_2 are the momentum fractions of the annihilating quark and antiquark. The leading protons are characterized by the Feynman variables x_F, when only one leading proton is observed, x_{F1} and x_{F2}, when both leading protons are observed.

The joint lepton-leading proton production proceeds as indicated in Figure 7. We write for the cross section to observe the lepton pair and one leading proton (in forward direction)

$$M^3 \frac{d^3\sigma}{dM dx_M dx_F} = W_1(\tau, x_M, x_F) = \frac{8\pi\alpha^2}{9} \frac{x_1 x_2}{\sqrt{x_M^2 + 4\tau}} \quad x$$

$$\cdot \sum_i Q_i^2 \left[F_{qi}(x_1) F_{\bar{q}i}(x_2) H_i\left(\frac{x_F}{1-x_1}, x_1\right) \right.$$

$$\left. + F_{\bar{q}i}(x_1) F_{qi}(x_2) H_{\bar{i}}\left(\frac{x_F}{1-x_1}, x_1\right) \right] \tag{4.3}$$

with the following definitions of the variables x_1 and x_2

$$x_{1,2} = \frac{1}{2}\left[\sqrt{x_M^2 + 4\tau} \pm x_M \right] \tag{4.4}$$

The proton recombination function $H_i(x, x_1)$ in (4.3) is defined in (3.4).

The cross section to observe the lepton pair and both leading protons is

$$M^3 \frac{d^4\sigma}{dM, dx_M dx_{F1} dx_{F2}} = W_2(\tau, x_M, x_{F1}, x_{F2}) = \frac{8\pi\sigma^2}{9} \frac{x_1 x_2}{\sqrt{x_M^2 + 4\tau}}$$

$$\cdot \sum Q_i^2 \left[F_{qi}(x_1) F_{\bar{q}i}(x_2) H_i\left(\frac{x_{F1}}{1-x_1}, x_1\right) H_{\bar{i}}\left(\frac{x_{F2}}{1-x_2}, x_2\right) \right.$$

$$\left. + F_{\bar{q}i}(x_1) F_{qi}(x_2) H_{\bar{i}}\left(\frac{x_{F1}}{1-x_1}, x_1\right) H_i\left(\frac{x_{F2}}{1-x_2}, x_2\right) \right] \tag{4.5}$$

In order to present and discuss the features of the leading proton-lepton pair correlations, we introduce again suitably defined divided correlations functions (defined here without the -1 term present in (3.5)).

$$R_1(\tau, x_M, x_F) = \frac{W_1(\tau, x_M, x_F)}{M^3 \frac{d^2\sigma}{d_M dx_M} \cdot \frac{d\sigma}{\sigma dx_F}} \tag{4.6}$$

and

$$R_2(\tau, x_M, x_{F1}, x_{F2}) = \frac{W_2(\tau, x_M, x_{F1}, x_{F2})}{M^3 \frac{d^2\sigma}{dM dx_M} \cdot \frac{d\sigma}{\sigma dx_{F1}} \cdot \frac{d\sigma}{\sigma dx_{F2}}} \tag{4.7}$$

As in Section 3, part of the correlation is due to kinematic effects and part is due to the quark-dynamics of the process. We do not try to separate both effects since we do not discuss alternative mechanisms to the Drell-Yan process.

In Figure 8 we present the correlation R_1 defined in (4.6). R_1 is plotted vs. x_F in Figure 8a for fixed $\tau = 0.12$ and different values of x_M, in Figure 8a for fixed $x_M = 0.2$ and different values of τ. The behaviour of the correlation is easy to understand qualitatively; when both the dilepton pair and the leading particle are required to move in forward direction (Figure 8a, $x_M = 0.4$) the production is strongly suppressed, the forward moving lepton pair is created from the valence quark of the forward moving incoming proton, therefore the secondary proton requires one sea quark. If the lepton pair moves opposite to the leading proton (Figure 8a, $x_M = -0.2, -0.4$), the lepton pair is formed from the valence quark of the incoming backward moving proton, all three valence quarks are available for the secondary forward moving proton, the production is not suppressed by the dynamics, however, we see the influence of energy momentum conservation, which restricts the allowed x_F range. In Figure 8b it is visible, how the kinematics suppresses the production if the lepton pair becomes more heavy.

In Figure 9 we show some features of the correlation function R_2, defined in (4.7) where both leading protons are observed. Figure 9a shows R_2 vs. x_{F1} for fixed τ and x_{F2} and different x_M values. Figure 9b shows R_2 vs. x_{F1} for different τ and x_{F2} values and fixed x_M. The qualitative behaviour or R_2 can be understood in a similar way as discussed above for R_1.

We conclude, the observation of such correlations provides a valuable test of the valence quark dynamics of the Drell-Yan process.

V. CONCLUSIONS

Further evidence has been presented for the quark recombination mechanism of leading particle production in hadron hadron collisions. The agreement with proton, neutron and Λ distributions in proton proton collisions is encouraging. Many

details of the quark recombination process are, however, not yet understood.

The correlations between leading particles and large transverse momentum particles or massive lepton pairs open a new way to test the underlying quark parton model for these processes. The agreement between the model calculations and the data available so far allows the optimistic conclusion that leading particle production as well as hard scattering processes can be understood in the quark-parton model. Further tests are, however, necessary. Experimental data are needed for such correlations involving heavy lepton pairs and new heavy particle production. Data for identified leading particles as well as identified large $p_\perp$ triggers are needed.

On the phenomonological and theoretical side further progress is needed. These correlations should be calculated in other competing models, for collisions involving different primary particles and leading particles. A more profound understanding of the quark recombination process and of the hard scattering process leading to large $p_\perp$ particles is needed.

ACKNOWLEDGEMENT

The author gratefully acknowledges the warm hospitality offered to him by Professor S. D. Drell in the Theory Group of SLAC. He would like to thank Dr. H. I. Miettinen, Dr. T. A. DeGrand, and Dr. S. J. Brodsky for valuable discussions.

REFERENCES

1. For recent reviews see D. Sivers, S. J. Brodsky, R. Blankenbecler, Phys. Rev. 23, 7 (1976); G. Ranft, J. Ranft, Leipzig preprint KMU-HEP-77-04 (1977) (to be published); S. D. Ellis, R. Stroynowski, Stanford Linear Accelerator Center preprint, SLAC-PUB-1903 (1977); G. C. Fox, Cal-Tech preprint, CAL-68-573 (1977); M. K. Chase, W. J. Stirling, University of Cambridge preprint, DAMTP 77/15 (1977).

2. S. M. Berman, J. D. Bjorken and J. Kogut, Phys. Rev. D4, 3358 (1971).

3. S. D. Ellis, M. B. Kislinger, Phys. Rev. D9, 2027 (1974).

4. B. L. Combridge, J. Kripfganz and J. Ranft, CERN preprint, CERN-TH-2343 (1977) (to be published in Physics Letters).

5. R. Cutler, D. Sivers, Argonne preprint, ANL-HEP-PR-77-40 (1977).

6. R. D. Field, R. P. Feynman, Phys. Rev. D15, 2590 (1977); R. P. Feynman, R. D. Field, G. C. Fox, Cal-Tech. preprint CALT-68-595.

7. J. Kripfganz, J. Ranft, Nucl. Phys. B124, 351 (1977); E. M. Ilgenfritz, J. Kripfganz, H. J. Möhring, G. Ranft, J. Ranft, A. Schiller, Leipzig preprint, KMU-HEP-77-01 (1977); A. Schiller, E. M. Ilgenfritz, J. Kripfganz, H. J. Möhring, G. Ranft, J. Ranft, Leipzig preprint, KMU-HEP-77-02 (1977).

8. L. Van Hove, S. Pokorski, Nucl. Phys. B86, 243 (1975).

9. H. Goldberg, Nucl. Phys. B44, 149 (1972); W. Ochs, Cal- Tech. preprint, CALT-68-542 (1976); R. Blankenbecler, S. J. Brodsky, Phys. Rev. D10, 2973 (1974); S. J. Brodsky, N. Weiss, SLAC preprint, SLAC-PUB-1926 (1977); S. J. Brodsky, J. F. Gunion, SLAC preprint, SLAC-PUB-1939 (1977).

10. K. P. Das, R. C. Hwa, Phys. Letters 68B, 459 (1977).

11. British-French-Scandinavian Collaboration, data presented by H. Bøggild at Symposium on Multi-Particle-Production, Kayserberg, France, June 1977, and private communication by M. G. Albrow (1977).

12. S. D. Drell, T. M. Yan, Phys. Rev. Letters 25, 316 (1970).

13. R. F. Peierls. T. L. Trueman, Ling-Lie Wang, Brookhaven National Laboratory preprint, BNL-22628 (1977); C. Quigg, Fermilab preprint (1977); K. Kajantie, Helsinki preprint HU-TFT-13-77 (1977); Review talk at European Conference on Particle Physics, Budapest 1977.

14. R. McElhaney. S. F. Tuan, Phys. Rev. D8, 226 7 (1973).

15. V. Barger. R. J. N. Phillips, Nucl. Phys. B73, 269 (1974).

16. J. W. Chapman, J. W. Cooper, N. Green, A. A. Seidl, J. C. Vander Velde, C. M. Bromberg, D. Cohen, T. Ferbel, P. Slattery, Phys. Rev. Letter 32, 260 (1974).

17. a) V. V. Ammosov, V. A. Gapienko, P. F. Ermolov, V. I. Koreshev, A. M. Moiseev, V. I. Sirotenko, E. A. Sloboduk, J. Derre, M. A. Jabiol, E. Pauli, M. Boratov, J. Loskiewicz, A. M. Touchard, Nucl. Phys. B115, 269 (1976).

b) J. W. Chapman, J. Cooper, N. Green, B. P. Roe, A. A. Seidl, J. C. Vander Velde, C. M. Bromberg, D. Cohen, T. Ferbel, P. Slattery, Phys. Letters 47B, 465 (1973).

c) K. Jaeger, D. Colley, L. Hyman, J. Rest, Phys. Rev. D77,2405 (1975).

d) A. Sheng, V. Davidson, A. Firestone, F. Nagy, C. Peck, F. T. Dao, R. Hanft, J. Lach, E. Malamud, F. Nezrick, A. Dzierba, R. Poster, Phys. Rev. D77, 1733 (1975).

18. M. G. Albrow, A. Bagchus, D. P. Barber, A. Bogaerts, B. Bosnjakovic, J. R. Brooks, A. B. Clegg, F. C. Erné, C. N. P. Gee, D. H. Locke,

F. K. Loebinger, P. G. Murphy, A. Rudge, J. C. Sens, F. Van der Veen, Nucl. Phys. B54, 6 (1973).

19. J. Engler, B. Gibbard, W. Isenbeck, F. Monning, J. Moritz, K. Pack, K. H. Schmidt, D. Wegener, W. Bartel, W. Flauger, H. Schopper, Nucl. Phys. B84, 70 (1975).

20. T. DeGrand, H. I. Miettinen (to be published).

21. For a review see J. Ranft, Fortschr. Phys. 23 467 (1975).

22. J. D. Bjorken, Lecture at SLAC Summer Institute (1975).

23. S. D. Ellis, M. Jacob, P. Landshoff, Nucl. Phys. B108, 93 (1976).

24. J. Ranft. G. Ranft. Nucl. Phys. B110, 493 (1976).

FIGURE CAPTIONS

1. Comparison of the leading proton and Λ hyperon production cross section $d\sigma/dx$ calculated according to Eq. (2.12) with data from Chapman et al.[16] for proton production at 102 and 404 GeV and with data on Λ-production at 69 GeV/c[17a], 102 GeV/c[17b], 205 GeV/c[17c], and 200 GeV/c[17d].

2. Comparison of the leading proton and neutron production cross section $E\, d^3\sigma/d^3p$ at fixed transverse momentum calculated according to Eq. (2.12) and assuming factorization between the x and $p_\perp$ dependence with data from Albrow et al.[18] for proton production at $s = 31$ GeV and from Engler et al.[19] for neutron production at $s = 30$ to 53 GeV.

3. Joint production of leading protons by quark recombination and large $p_\perp$ quark jets by hard quark-quark scattering. Valence quarks are denoted by V_i, sea quarks by s_i. The scattered quark is a valence quark in Figure 3a, a sea quark in Figure 3b. The process of Figure 3b alone is used to estimate the kinematic contribution to the correlation between leading protons and large $p_\perp$ jets.

4. Comparison of the leading proton--large $p_\perp$ -u and d quark jet correlation function $R(p_\perp, y, x)$ according to Eq. (3.5), plotted as function of the leading proton Feynman x variable for different jet (pion) transverse momenta, with data of the British-French-Scandinavian collaboration[11] from positively and negatively charged large $p_\perp$ triggers (a) The full correlation function including the dynamic and kinematic contributions, (b) the kinematical correlation only, calculated according to the process in Figure 3b.

5. Comparison of the leading proton--large $p_\perp$ jet correlation function $R(p_\perp, y, x)$ according to Eq. (3.5), plotted as functions of the jet (pion)

transverse momentum for different Feynman x of the leading proton with data of the British-French-Scandinavian collaboration.[11]
(a) The full correlation function including the dynamical and kinematic contributions (b) The kinematical correlation only, calculated according to the process in Figure 3b.

6. The leading proton--large $p_\perp$ jet correlation function plotted as function of the jet transverse momentum for different leading proton x values and for c.m.s. jet rapidities $y_3 = 0$, 1, and 2.

7. Joint production of two leading protons by the quark recombination process and of one heavy lepton pair by the Drell-Yan mechanism.

8. The correlation function $R_1(\tau, x_M, x_F)$ between one massive lepton pair and one leading proton. (a) Plotted vs. the Feynman variable x_F of the leading proton for $\tau = 0.12$ and different x_M of the lepton pair. (b) Plotted vs. x_F for $x_M = 0.2$ and different values of τ.

9. The correlation function $R_2(\tau, x_M, x_{F1}, x_{F2})$ between two leading protons and one massive lepton pair. (a) Plotted vs. x_{F1} for constant τ and x_{F2} for different values of x_M. (b) Plotted as function of x_{F1} for $x_M = 0$ and different values of τ and x_{F2}.

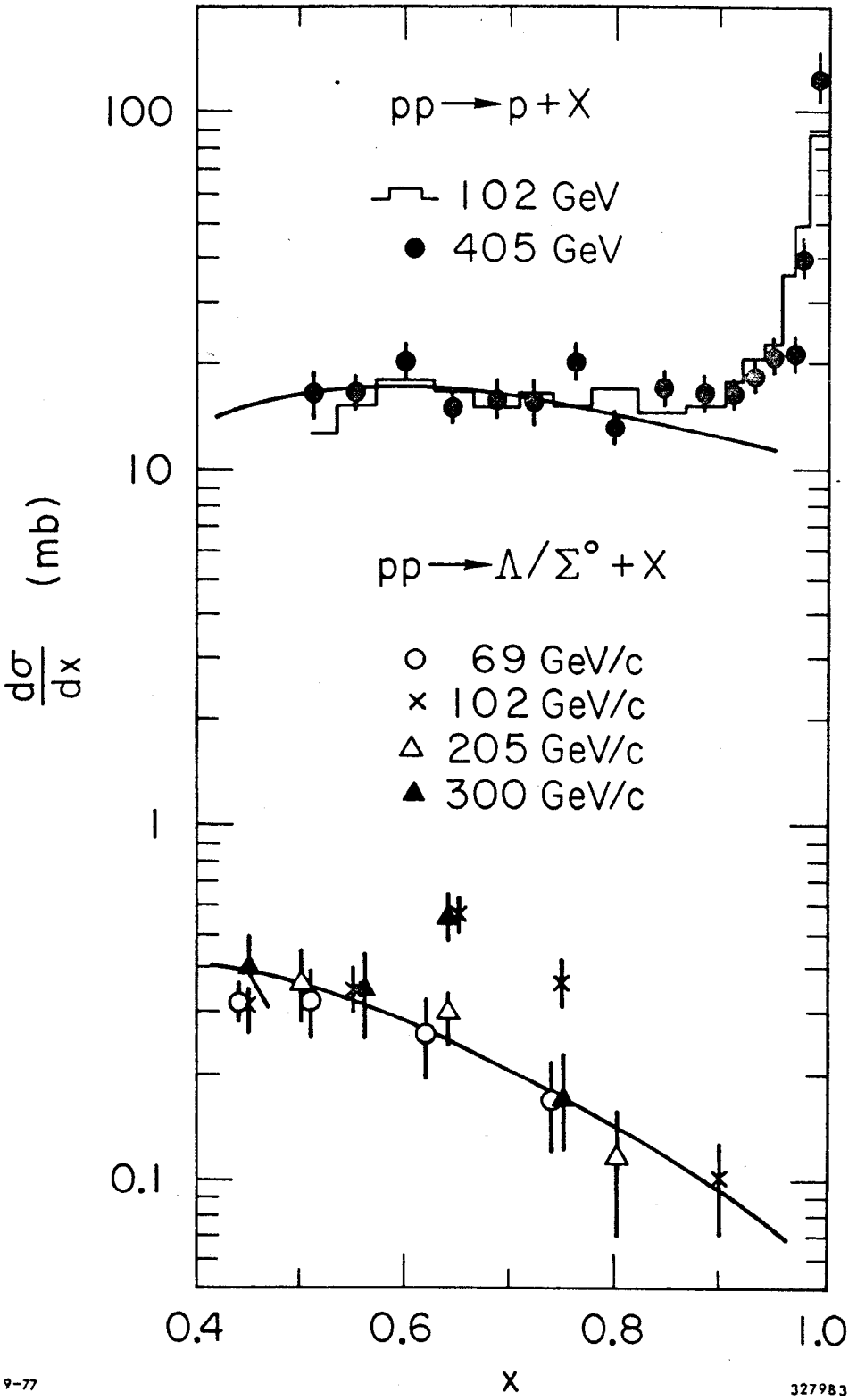
100
10
1
0.1
pp → p + X
102 GeV
405 GeV
pp → Λ/Σ° + X
69 GeV/c
102 GeV/c
205 GeV/c
300 GeV/c
dσ/dx (mb)
0.4
0.6
0.8
1.0
x
9-77
327983

Fig 1

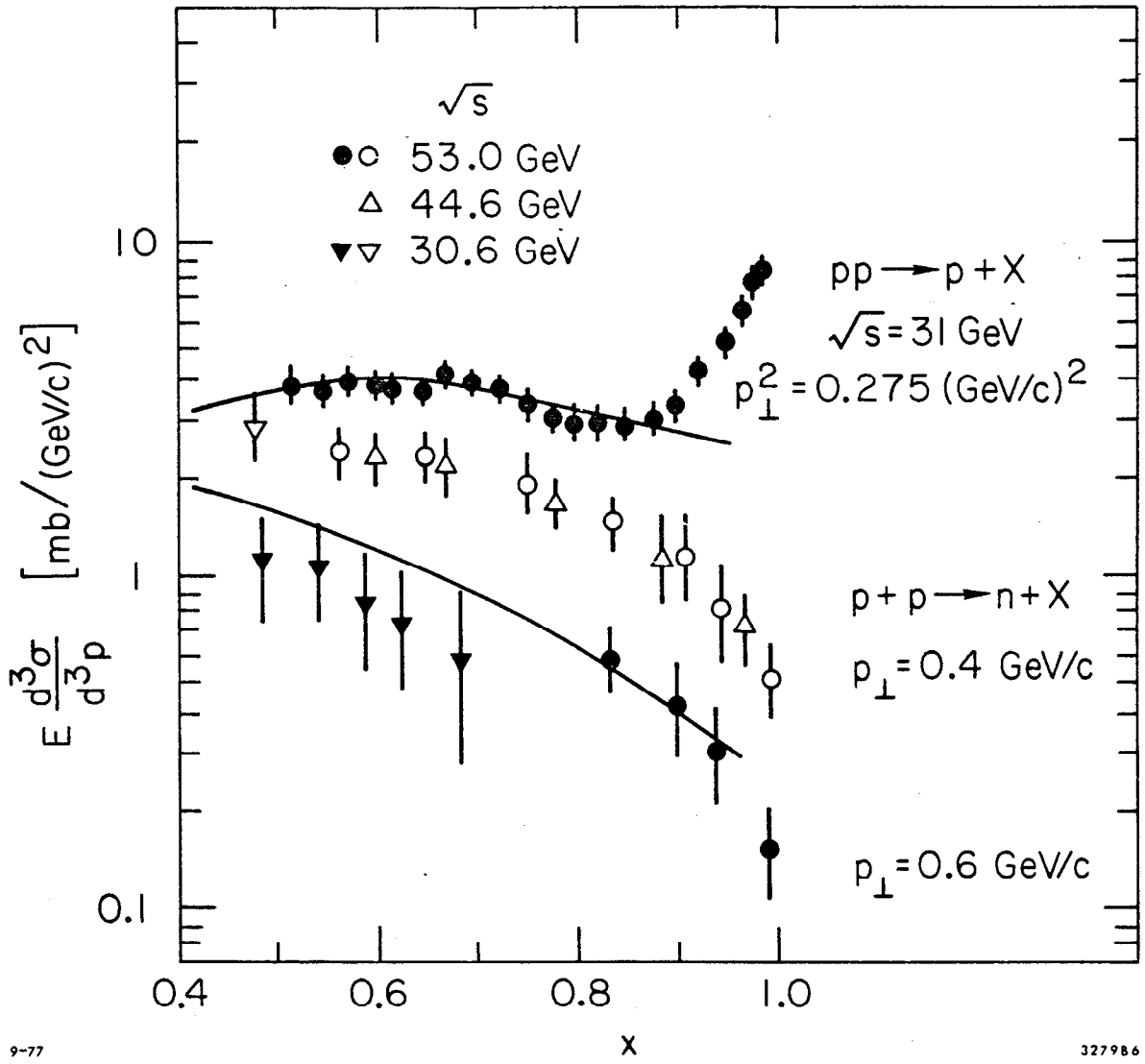
√s
53.0 GeV
44.6 GeV
30.6 GeV
pp → p + X
√s = 31 GeV
p⊥² = 0.275 (GeV/c)²
p + p → n + X
p⊥ = 0.4 GeV/c
p⊥ = 0.6 GeV/c
E d³σ/d³p [mb/(GeV/c)²]
10
1
0.1
0.4
0.6
0.8
1.0
x
9-77
327986

Fig 2

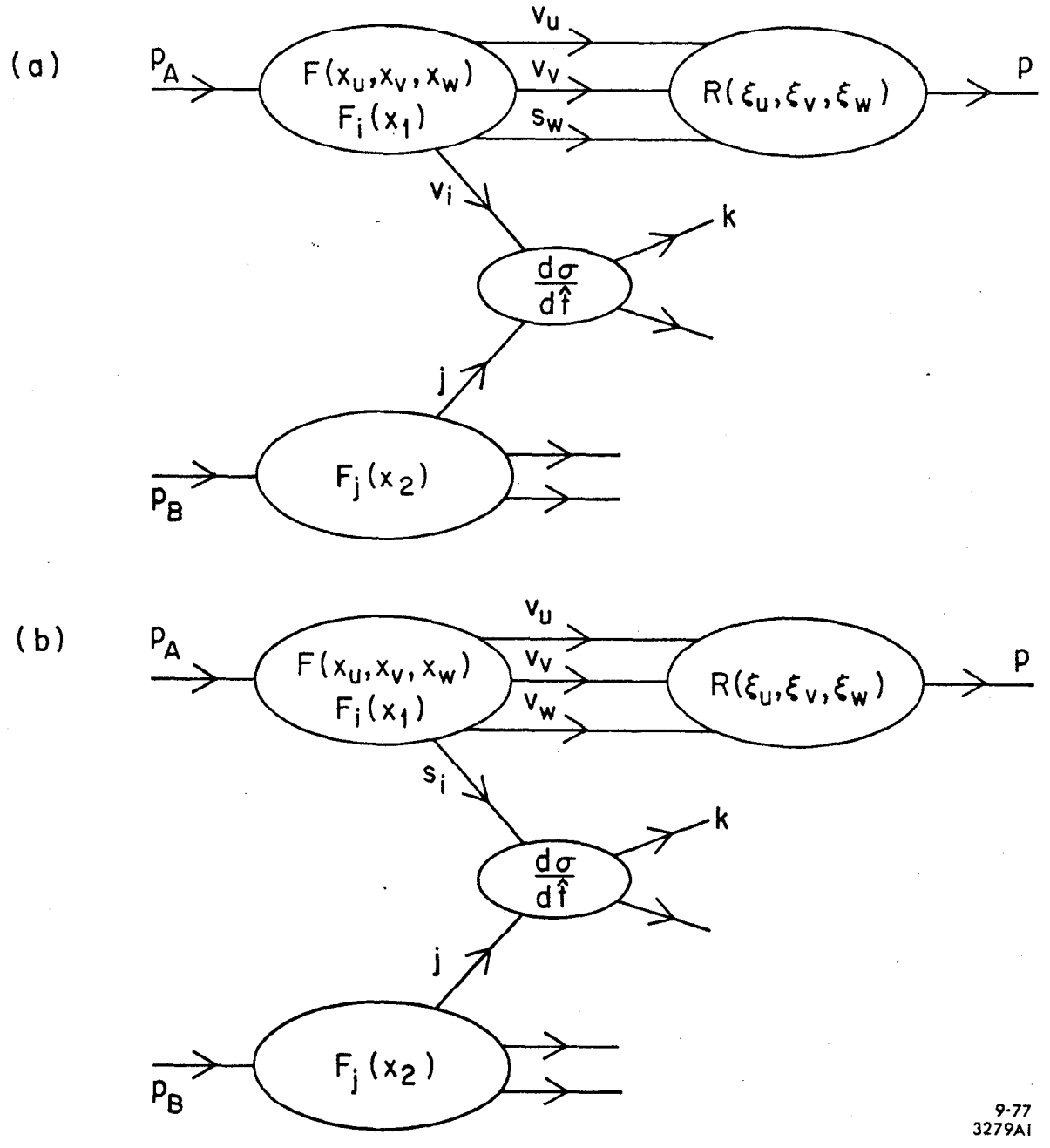
(a)
p_A
$F(x_u, x_v, x_w)$
$F_i(x_1)$
v_u
v_v
s_w
$R(\xi_u, \xi_v, \xi_w)$
p
v_i
k
$\frac{d\sigma}{d\hat{t}}$
j
$F_j(x_2)$
p_B
(b)
p_A
$F(x_u, x_v, x_w)$
$F_i(x_1)$
v_u
v_v
v_w
$R(\xi_u, \xi_v, \xi_w)$
p
s_i
k
$\frac{d\sigma}{d\hat{t}}$
j
$F_j(x_2)$
p_B
9-77
3279A1

Fig 3

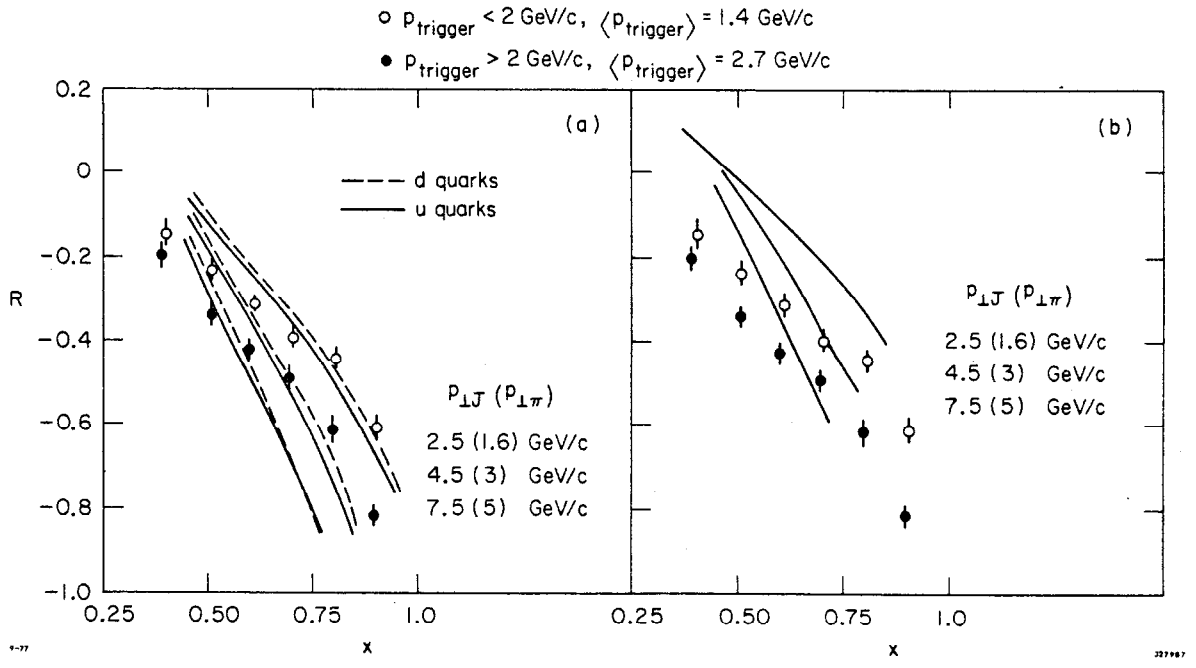
o $p_{trigger} < 2$ GeV/c, $\langle p_{trigger} \rangle = 1.4$ GeV/c
• $p_{trigger} > 2$ GeV/c, $\langle p_{trigger} \rangle = 2.7$ GeV/c
(a)
(b)
d quarks
u quarks
$p_{\perp J}$ ($p_{\perp \pi}$)
2.5 (1.6) GeV/c
4.5 (3) GeV/c
7.5 (5) GeV/c
R
x
0.2
0
-0.2
-0.4
-0.6
-0.8
-1.0
0.25
0.50
0.75
1.0

Fig. 4

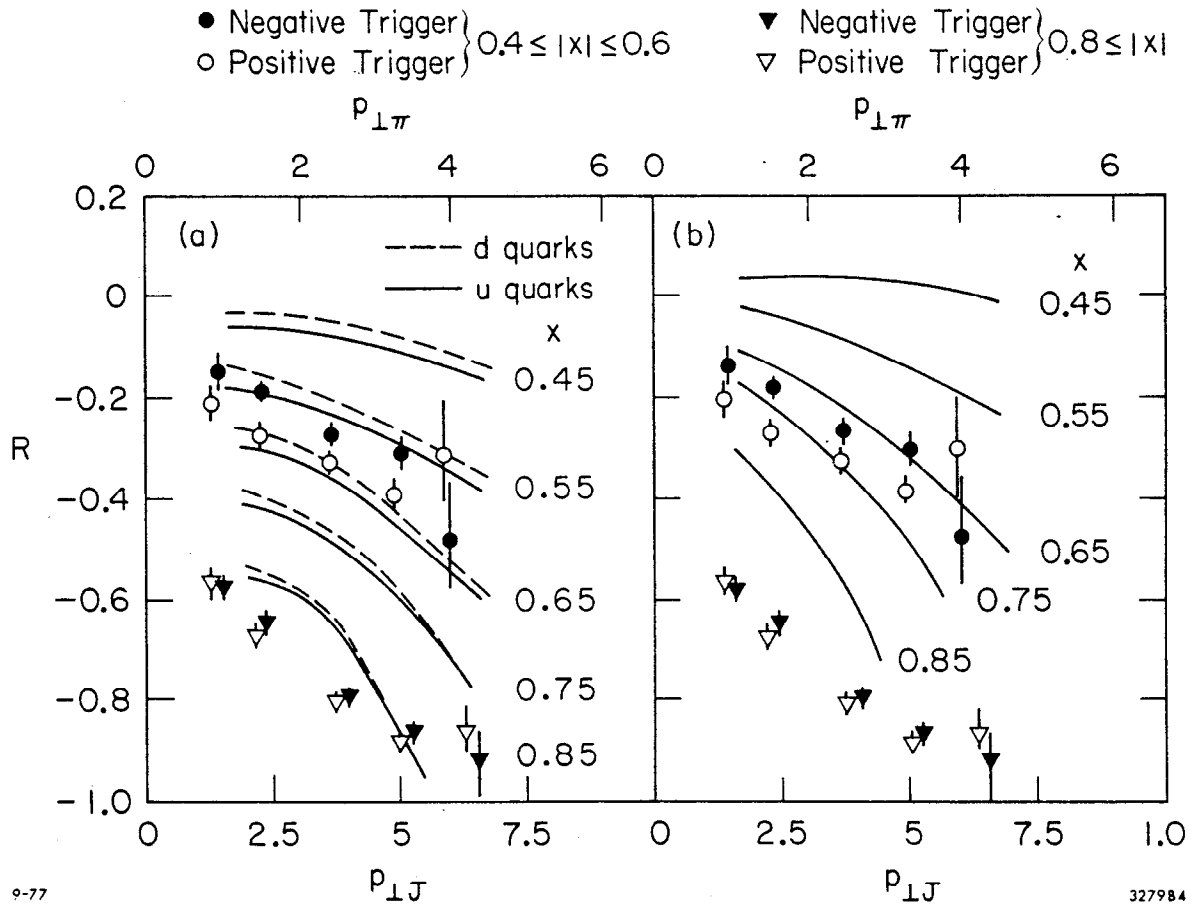
● Negative Trigger
○ Positive Trigger
0.4 ≤ |x| ≤ 0.6
▼ Negative Trigger
▽ Positive Trigger
0.8 ≤ |x|
$p_{\perp\pi}$
(a)
(b)
d quarks
u quarks
x
0.45
0.55
0.65
0.75
0.85
R
$p_{\perp J}$
9-77
327984

Fig 5

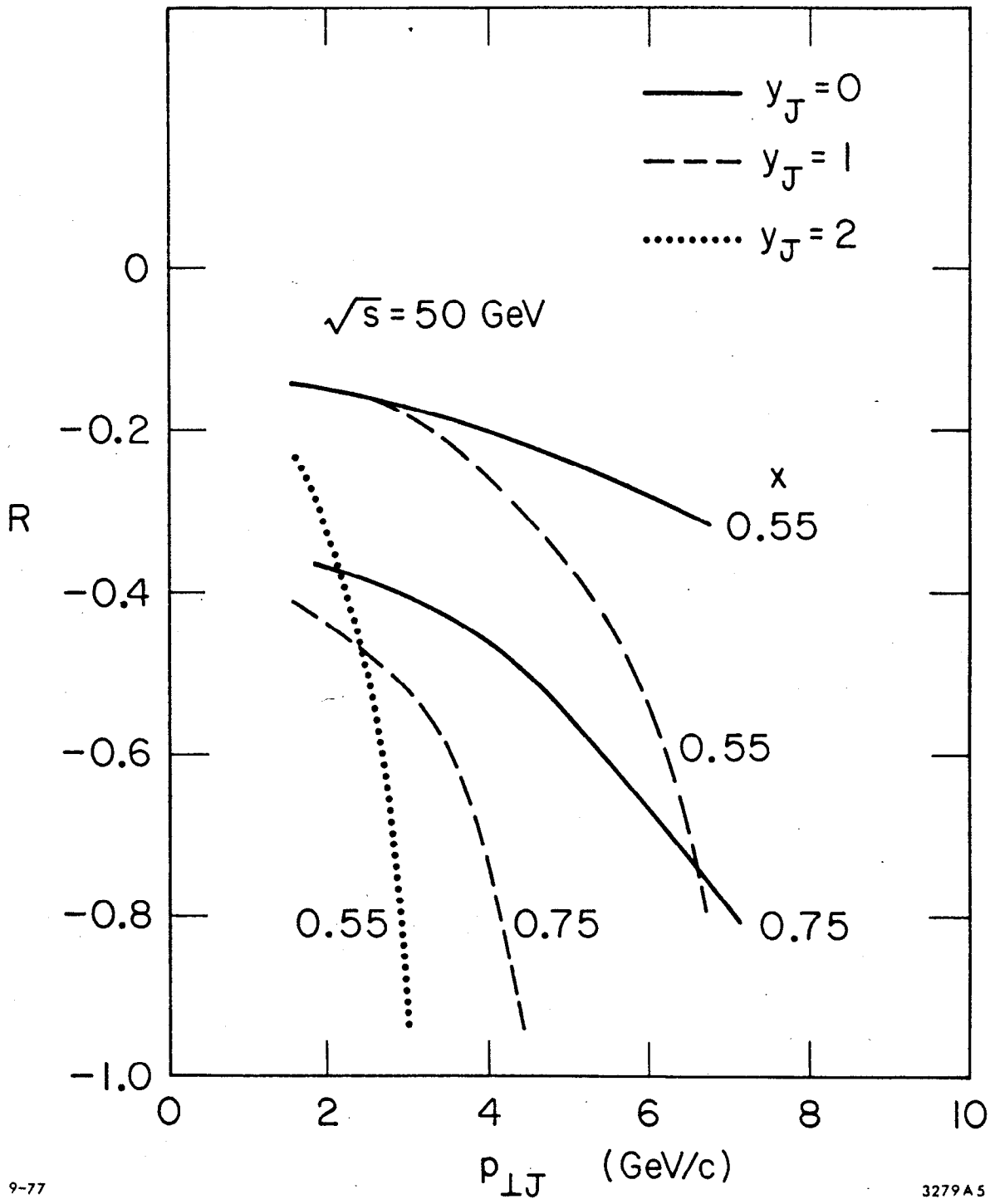
$y_J = 0$
$y_J = 1$
$y_J = 2$
$\sqrt{s} = 50$ GeV
x
0.55
0.55
0.55
0.75
0.75
R
0
-0.2
-0.4
-0.6
-0.8
-1.0
0
2
4
6
8
10
$p_{\perp J}$ (GeV/c)
9-77
3279A5

Fig. 6

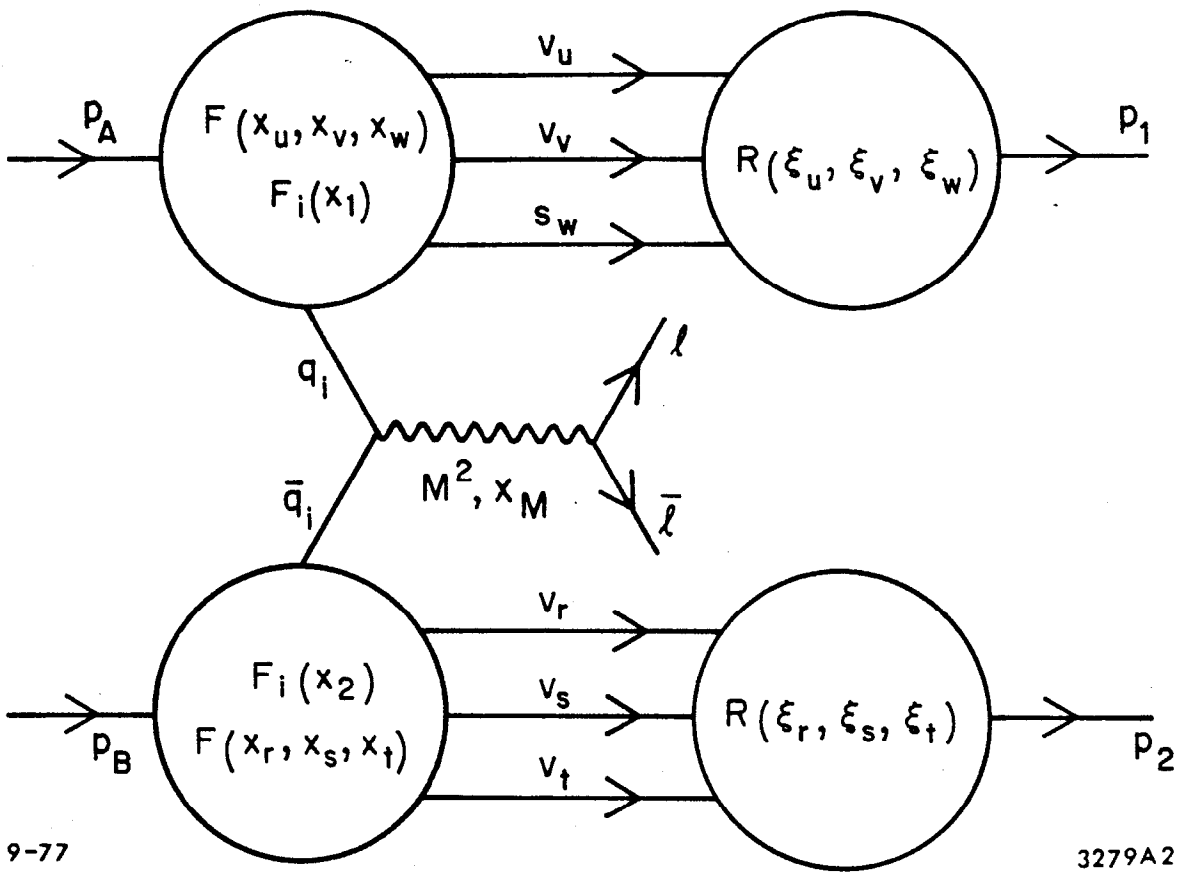
p_A
$F(x_u, x_v, x_w)$
$F_i(x_1)$
v_u
v_v
s_w
$R(\xi_u, \xi_v, \xi_w)$
p_1
q_i
$\bar{q}_i$
M^2, x_M
ℓ
$\bar{\ell}$
p_B
$F_i(x_2)$
$F(x_r, x_s, x_t)$
v_r
v_s
v_t
$R(\xi_r, \xi_s, \xi_t)$
p_2
9-77
3279A2

Fig. 7

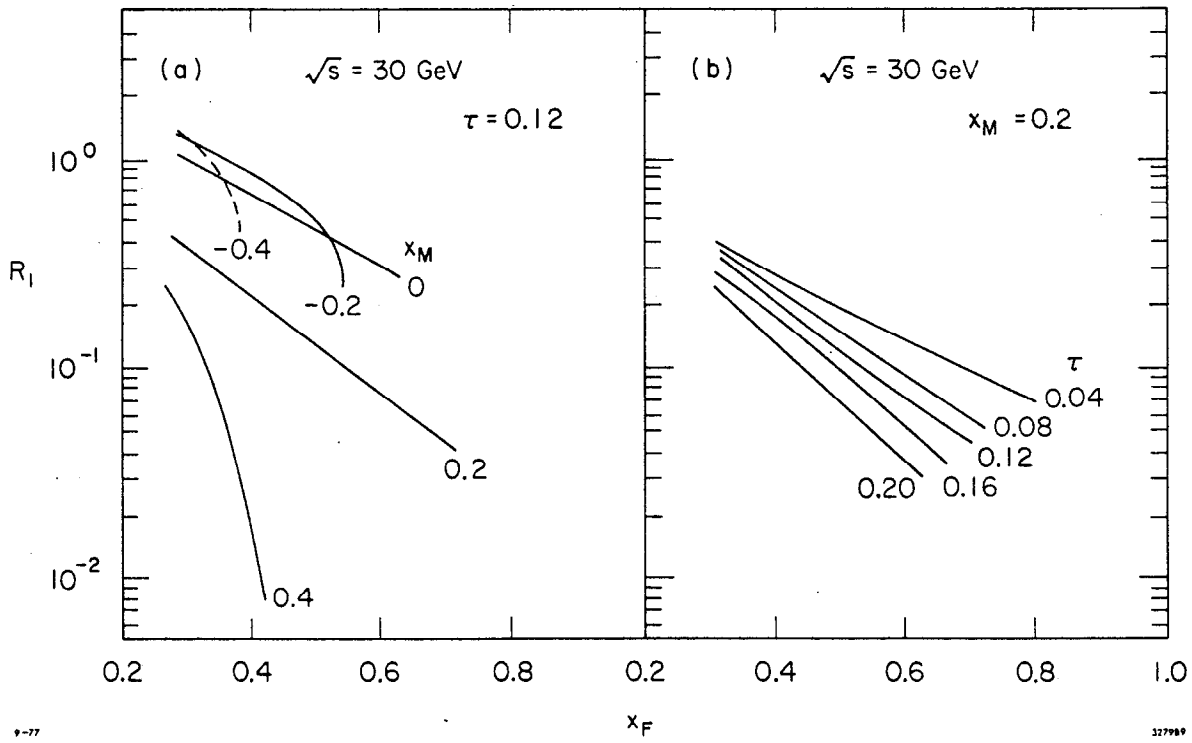
(a)
$\sqrt{s}$ = 30 GeV
τ = 0.12
(b)
$\sqrt{s}$ = 30 GeV
x_M = 0.2
R_1
10^0
10^{-1}
10^{-2}
x_M
-0.4
-0.2
0
0.2
0.4
τ
0.04
0.08
0.12
0.16
0.20
0.2
0.4
0.6
0.8
1.0
x_F

Fig 8

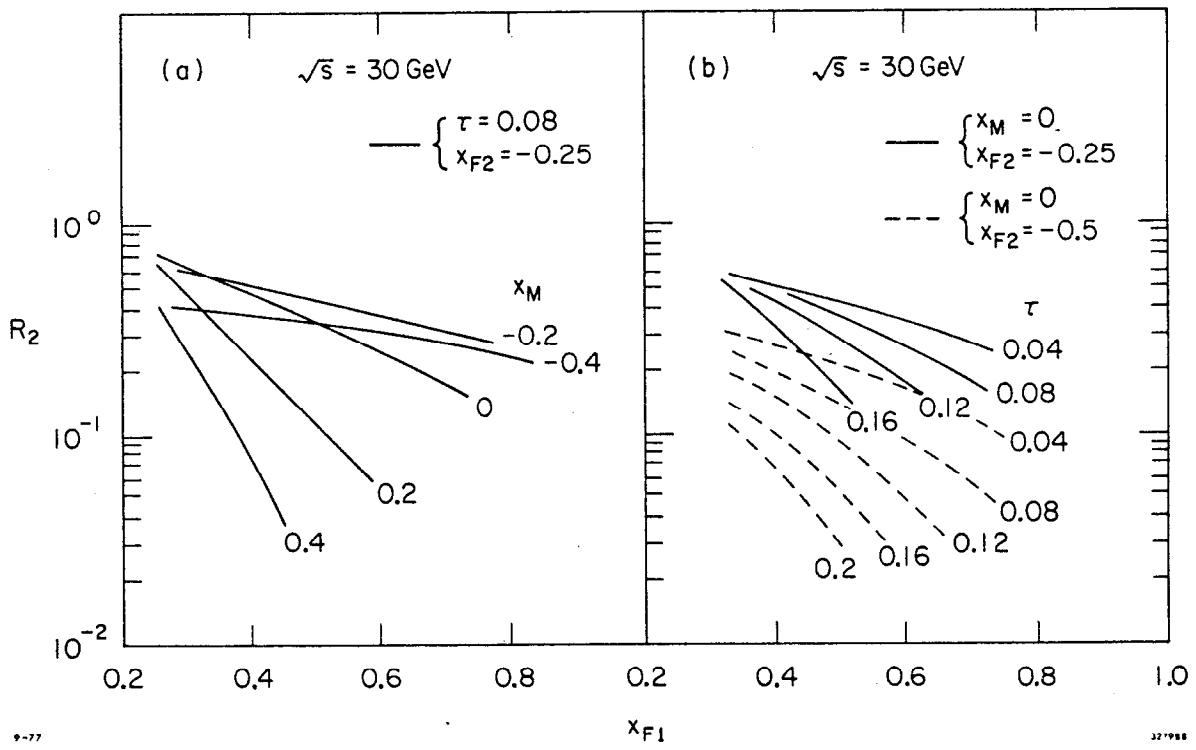
(a)
$\sqrt{s}$ = 30 GeV
τ = 0.08
x_{F2} = −0.25
x_M
−0.2
−0.4
0
0.2
0.4
(b)
$\sqrt{s}$ = 30 GeV
x_M = 0
x_{F2} = −0.25
x_M = 0
x_{F2} = −0.5
τ
0.04
0.08
0.12
0.16
0.2
R_2
10^0
10^{-1}
10^{-2}
0.2
0.4
0.6
0.8
1.0
x_{F1}

Fig. 9